CRYM as an intracellular T3 holder *in vivo*.

Satoru Suzuki[1], Nobuyoshi Suzuki[2] , Jun-ichirou Mori[1], Aki Oshima[2], Shinichi Usami[2], Kiyoshi Hashizume[1]

1. Department of Aging Medicine and Geriatrics, Institute on Aging and Adaptation, Shinshu University, Graduate School of Medicine, 3-1-1, Asahi, Matsumoto, 390-8621, JAPAN,

2. Department of Otorhinolaryngology, Shinshu University School of Medicine, 3-1-1, Asahi, Matsumoto, 390-8621, Japan

running title in vivo function of CRYM

key words: CRYM, thyroid hormone, knockout mice, deafness, crystallin

Correspondence should be addressed to Satoru Suzuki, M.D., Ph.D., Department of Aging Medicine and Geriatrics, Institute on Aging and Adaptation, Shinshu University, Graduate School of Medicine, 3-1-1, Asahi, Matsumoto, Nagano, 390-8621, Japan

TEL: +81-263-37-2686

FAX: +81-263-37-2710 E-MAIL: soutaro@hsp.md.shinshu-u.ac.jp

Disclosure statement: The authors have nothing to disclose.

Abstract

Previously, we identified NADPH-dependent cytosolic T3 binding protein (CTBP) in rat cytosol. CTBP is identical to μ-crystallin (CRYM). Recently, CRYM mutations were found in patients with non-syndromic hereditary deafness. Although it has been established that CRYM plays pivotal roles in reserving and transporting T3 into the nuclei *in vitro* and has a clinical impact on hearing ability, the precise functions of CRYM remain to be elucidated *in vivo*.

To further investigate the *in vivo* functions of *CRYM* gene products, we have generated mice with targeted disruption of the *CRYM* gene, which abrogates the production of CRYM. CRYM knockout loses the NADPH-dependent T3 binding activity in the cytosol of the brain, kidney, heart, and liver. At the euthyroid state, knockout significantly suppresses the serum concentration of T3 and T4 despite normal growth, heart rate and hearing ability. The disruption of the gene does not alter the expression of TSHβ mRNA in the pituitary gland or glutathione S transferase alpha 2 and deiodinase 1 mRNAs in either the liver or kidney. When radiolabeled T3 is injected intravenously, labeled T3 rapidly enters into then escapes from the tissues in CRYM-knockout mice. These data suggest that because of rapid T3 turnover, disruption of the CRYM gene decreases T3 concentrations in tissues and serum without alteration of peripheral T3 action *in vivo*.

Introduction

The variety of effects on growth, development, and metabolism attributable to thyroid hormone suggests that this hormone acts through a fundamental mechanism common to many different tissues, yet is capable of multiple functions (1). The pivotal action of T3 is initiated through binding to its nuclear receptors in the target tissues (2). Following secretion of the hormone from thyroid gland, T3 travels a long distance to the target. Thyroid hormone moves from outside the plasma membrane into the extra-nuclear space of the cells through active transporters or by passive diffusion (3). Although many studies demonstrated that cytosolic T3 binding proteins are present *in vitro*, little is known about the molecular mechanisms of T3 retention in cytoplasm, especially, the physiological roles of cytosolic T3 *in vivo* (4).

In 1986, it was reported that charcoal treatment of rat renal cytosol abolishes the hormone binding activity, while the addition of NADPH restores it (5). Two proteins were identified. One was purified from rat kidney (6) and brain (7), and showed a molecular mass of 58kDa. The other was obtained from rat liver (8), astroglial cells (9), and human kidney (10), and showed a molecular mass of 38kDa. The latter was identified as μ-crystallin (CRYM), which was initially cloned from kangaroo lens (11)(12). CRYM is a taxon-specific protein which is particularly abundant in kangaroo lens, not in mouse or other mammals (13). Our previous study demonstrated that CRYM held T3 in cytoplasm, which increased the T3 concentration in both whole cells and the nuclei in CRYM-expressing GH3 cells (14). However, expression of CRYM suppressed transactivity mediated by T3 in the same cell lines.

Recently, it was reported that CRYM is abundant in cochlear and vestibular tissues in the inner ear (15). Immunohistochemical study demonstrated that the protein was preferentially expressed in fibrocyte type 2 where Na-K ATPase is enriched (16). Two patients with non-syndromic deafness were reported to be associated with point mutations in the *CRYM* gene (15). In a study assessing NADPH-dependent T3 binding to the two reported mutations (16), one mutation, T314Y abolished NADPH-dependent T3 binding, while the other did not influence the binding activity. The proband with T314Y showed

severe hearing loss, while the patient with X314T demonstrated moderately impaired hearing. It is suggested that the thyroid hormone binding property may relate to the development of hearing impairment in patients with the CRYM mutations.

To clarify the physiological roles of CRYM *in vivo*, we generated mice in which the *CRYM* gene was disrupted. We assessed the phenotypes, especially the heart rate, hearing ability, kinetics of the thyroid hormone, serum concentrations of thyroid hormones and the mRNA expression of the thyroid hormone response genes.

Results

Production of mice with inactivated CRYM

To inactivate the *CRYM* gene, a recombination cassette containing a NeoR gene driven by mouse phosphoglycerate kinase promoter was introduced in the first and second coding exons (Fig1a). The mutated allele was introduced into the *CRYM* locus by homologous recombination in embryonic stem (ES) cells. Heterozygous mice were derived from an inbred C57BL6 background. The chimeric mouse was mated to 129Sv mice and then back-crossed 6 times into the same strain, diluting the C57BL6 background.

Expression of CRYM gene

Northern blotting demonstrated a single 2.2kb band in the lane applied brain total RNA from the wild (CRYM+/+) mice (left panel in Fig1b). The signal was attenuated in the lane of the CRYM+/- mice. There was no signal detected in the CRYM-/- mice. Western blotting showed a single 38-kDa band in the CRYM+/+ and CRYM+/- mice, but not in the CRYM-/- mice (right panel in Fig1b).

NADPH-dependent T3 binding activity

NADPH-dependent T3 binding was assessed in whole brain, heart, kidney and liver of the CRYM+/+ and CRYM-/- mice. As shown in Fig1c, there were no specific bindings to T3 in the charcoal-treated crude cytosol obtained from any of the tissues we studied (*black and shaded bars*). When we added NADPH to the charcoal-treated extracts, specific binding to T3 was observed in all tissues from the CRYM+/+ mice as previously demonstrated (*white and*

hatched bars) (17). These binding activities were abolished using extracts from the CRYM-/- mice. Scatchard analyses demonstrated that *Ka* in the CRYM+/+ mice was approximately 2 x 10^9/M (Fig1d). We could not calculate *Ka* in the CRYM-/- mice, because of the lack of specific binding.

Growth curve, heart beats and hearing ability

The mice were intercrossed to produce homozygous mutants. Among 155 pups born, 34 (22%), 87 (56%), and 34 (22%) were wild-type, heterozygous and homozygous progenies, respectively. These data show that homozygous disruption of the *CRYM* gene is not deleterious to embryonic development. The growth rate of heterozygous mice was similar to that of wild-type mice (Fig2a). Low and high heart rates were shown in wild-type mice fed a low iodide diet plus1% PTU and 1μg/ml T3 water *ad libitum*, respectively, as controls. There were no significant differences in the heart rates among CRYM+/+, CRYM+/-, or CRYM-/- mice, (Fig2b). To assess hearing, ABR was measured in CRYM+/+ and CRYM-/- littermates. The responses were apparently normal in CRYM-/- mice (Fig2c). The thresholds of CRYM-/- mice were not significantly different from those of CRYM+/+ mice (Fig2d).

Serum concentrations of T3, T4 and TSHβ mRNA expression in the pituitary gland.

We measured the serum concentrations of T3 and T4 in CRYM+/+, CRYM+/-, and CRYM-/- mice. As shown in Fig 3a, the concentrations of both T3 and T4 were significantly lower in the CRYM-/- mice than in CRYM+/+ mice. T3 and T4 concentrations were reduced by 13% and 25% in CRYM-/- mice, respectively. In contrast, there was no significant difference in TSHβ mRNA expression between the CRYM+/+ and the CRYM-/- mice. The data from the northern blotting were consistent with the findings obtained from the quantitated PCR (Fig3b). As shown in Fig3c, there were no apparent histological differences between CRYM +/+ and CRYM -/- mice in either the pituitary or thyroid gland.

mRNA levels of T3 responsive genes in the liver, kidney and heart

To evaluate peripheral activity induced by thyroid hormone in knockout mice, we measured the expressions of Gsta2 and Dio1 mRNAs in the liver and kidney and the expression of Dio1 mRNA in the heart. There were no significant differences in Gsta2 or Dio1 mRNA expression in either the liver or kidney

among CRYM+/+, CRYM+/- and CRYM-/- mice (Fig 4a). In the heart, the expression of Dio1 in CRYM+/+ mice was not different from that in CRYM-/- mice. The expression of Gsta2 was not performed since the expression was too low to evaluate in this system. Northern blotting also demonstrated similar results to the data using the quantitated PCR (Fig4b).

T3 kinetics in wild and homo-mice.

To investigate the physiological roles of CRYM *in vivo*, we injected labeled-T3 intravenously and measured the radioactivity in various tissues 1,2,4, and 8 hours post injection. In the CRYM+/+ mice, radioactivity in all tissues studied except for the brain gradually increased for two hours after injection, then slowly decreased until 8 hours post injection (Fig5a-d). In the brains of CRYM+/+ mice, it took 4 hours to reach the peak radioactivity. However, the radioactivities in all tissues peaked 1hour post injection, then sharply declined in the CRYM-/- mice. There were no significant changes in serum radioactivities between the CRYM+/+ and CRYM-/- until 8 hours post injection (Fig5e).

Discussion

In this study, we succeeded in disrupting the *CRYM* gene and omitting the expression of the protein *in vivo*. NADPH-dependent T3 binding activity was eliminated in the tissues we studied, suggesting that the CRYM protein is an unique protein among cytosolic proteins that are capable of binding to T3 in the presence of NADPH. We have reported two proteins of different molecular weights, which possess high affinity to T3 in the presence of NADPH in rat tissues. One was purified from rat kidney and showed a molecular weight of 4.7S, and mass of 58kDa (6). The other was isolated from rat liver and showed a molecular mass of 38KDa (8). The molecular weight was 5.1S, since this protein formed a dimer. Currently, we do not have evidence to explain why NADPH-dependent T3 binding completely vanished even though one of the proteins should have survived. CRYM protein may be affected by post-translational modification, such as glycosylation, myristoylation, or other processes. Such post-translational modification may alter the molecular weight. As a result, there are two molecular weights of the protein originating from a single protein. Furthermore, the antibody may not recognize the modified protein. These proteins have also been reported (18).

On the initial phenotypical assessment, there were no significant differences in terms of growth rate, heart rate, and hearing ability. Hearing is one of the most important functions controlled by thyroid hormone (19)(20). It is reported that CRYM mutations are associated with non-syndromic deafness. The disruption of the CRYM gene apparently does not alter the hearing function. From these data, the expression of abnormal CRYM proteins may affect the hearing function of the inner ear in patients with *CRYM* mutations. We suggest that the mutation that abolishes NADPH-dependent T3 binding causes severe impairment of the hearing as previously reported (16). Taken together, these data indicate that other factors, including thyroid hormone may also affect hearing loss.

In contrast to normal growth, heart rate, and hearing ability, disruption of the gene decreased the serum concentration of T3 without alteration of the TSHβ concentration in the pituitary gland. T4 concentration was also suppressed by the disruption of the gene. It was reported that the binding affinity of CRYM to T4 is approximately 5-10 times lower than that to T3 *in vitro* (8). These data suggest that CRYM disruption may suppress the T4 concentration directly, or through the feedback loop in TRH-TSH-thyroid axis indirectly *in vivo*. Because of the small change in the thyroid hormone concentration, we note the possibility that a correspondingly small change exists in the amount of TSHβ mRNA that has not been detected.

Gsta2 and Dio1 are reported to be negatively and positively regulated by T3, respectively (21)(22). Although the concentration of T3 and T4 were low in CRYM-/- mice, the expression level of T3 target genes was normal rather than low in CRYM-/- mice.

A previous study demonstrated that CRYM affected cellular retention of T3 in living cells (14). This observation presupposes that the disruption of the *CRYM* gene may alter the kinetics of T3 *in vivo*. We counted the radioactivity of the tissues after injection of the labeled T3 intravenously via the tail vein. Both the influx and efflux of radiolabeled T3 were increased in all of the tissues we studied in these knockout mice. These findings are consistent with the previous data obtained using the CRYM-expressing cells.

Up to the present, four cytosolic thyroid hormone binding proteins have

been reported, *i.e.* pyruvate kinase subunits (23), aldehyde dehydrogenase (24), glutathione-S-transferase (25) and CRYM. Although the affinity constants of these proteins to T3 are 8-34 times lower than that of CRYM, these proteins may have physiological functions for cytoplasmic T3 retention or transport. MCT8 or other T3 transporters in plasma membrane also contribute to the regulation of intracellular T3 concentration (26)(27).

CRYM proteins may have redundant functions. The protein binds not only T3 but also NADPH (28). Currently the physiological significance of this coupling is not known. Since NADP inhibits T3 binding, it is possible that oxidative metabolism is other factors for control of T3 binding to CRYM in cytoplasm (8).

In conclusion, we disrupted NADPH-dependent T3 binding following the elimination of CRYM expression. Normal growth, heart rate and hearing were observed. The expressions of TSHβ, Gsta2, and Dio1 were not changed by the disruption, although the serum concentration of thyroid hormone was altered. T3 rapidly entered into and escaped from the tissues. These data suggest that CRYM affects T3 kinetics *in vivo*, and that elimination affects the serum concentrations of T3 and T4 but not the apparent phenotype and peripheral thyroid hormone action in the euthyroid state. The precise molecular mechanism of CRYM action remains to be elucidated.

Materials and Methods

Generation of the CRYM knockout mouse

The CRYM knockout mouse was generated by in Genious Targeting Laboratory (Stony Brook, NY) on a commercial basis. The *CRYM* gene was cloned from a 129Sv genomic library (Stratagene, Cedar Creek) and was used to construct targeting vector containing the neomycin resistance gene flanked by two genomic fragments spanning the *CRYM* gene promoter, Exon 1 and 2 regions. The long fragment of the targeting construct was a 7.6-kilobase sequence upstream from Exon1. The short fragment of the targeting construct was 1.2-kilobase-long sequence downstream of Exon2. The targeted allele contained a deletion of the *CRYM* gene promoter, Exon1, and Exon2. IT2 embryonic stem cells were transfected with the targeting vector and incubated in

media containing G418. Surviving colonies were analyzed by PCR analysis to identify homologous recombinants. One correctly targeted embryonic stem cell clone was microinjected into C57BL/6J host blastocysts to generate chimeric mice, which were bred with C57BL/6J mice to obtain heterozygous offspring. Mouse genotyping was performed with genomic DNA isolated from toes using SDS/proteinase K solubilization. The wild type CRYM allele was identified by PCR using primers

a (5'-TGCATCCCTGAAGTGGGGTA-3')

and b (5'-GAATGAGCGCAAACGGAATG-3'), which amplified an 800-base product. The knockout allele was identified by PCR using primers a and c (5'-AGGCAGAGGCCACTTGTGTAG-3'), which amplified a 500-base product-containing fragment of the neomycin resistant cassette. Heterozygous mice were crossed with the 129Sv strain at least 6 times before they were interbred to generate homozygous knockout mice. The wild-type mice used in this study as controls were littermates of the knockout mice. Procedures carried out in mice were approved by Shinshu University Institutional Animal Care and Use Committee.

Northern and Western blotting

In Fig1, the brains were obtained from the 3-week-old mice for the Northern and Western analyses. Northern hybridization was performed by the standard procedures using random-primed full length CRYM fragment as a probe (27). In Fig3b and 4b, the pituitary gland, liver and kidney were obtained from the six-week-old male mice. Ten μg of the total RNA obtained from six pituitary glands was electrophoresed and hybridized with ^{32}P-labeled TSHβ or EF1 probe. Twenty μg of the total RNA obtained from 50mg liver or kidney was electrophoresed and hybridized with labeled Dio1, Gsta2, or EF1. A series of the mouse probes were obtained from PCR amplification of the reverse-transcribed poly A RNA extracted from the pituitary gland or liver. The following oligonucleotides were used.

TSHβ; sense 5'-GAACGGAGAGTGGGTCATCACA-3'

antisense 5'-AGTAGTTGGTTCTGACAGCCTC-3,

Dio1; sense 5'-TGTAGGCAAGGTGCTAATGAC-3',

antisense 5'-TGCCGGATGTCCACGTTGTTC-3',

Gsta2; sense 5’-GCAGAATGGAGTGCATCAGGT-3’
antisense 5’-TCTGCTCTTGAAGGCCTTCAGC-3’
EF1 sense 5’-CCATGAAGCTTTGAGTGAAGCTCT-3’
antisense 5’-TAGCCTTCTGAGCTTTCTGGGCAG-3’
Amplified fragment was sequenced and checked fidelity of the sequences. Western blotting was carried out by using anti-μ-crystallin antibody (Santacruz, CA).

Scatchard analysis

oScatchard analyses and NADPH-dependent T3 binding assays were performed as previously described (28). Briefly, tissues were homogenized and centrifuged to isolate the crude cytosolic fraction. The fraction was incubated with 1% charcoal to remove T3, NADPH, and other small molecules. After spinning down, the supernatant was incubated with [^{125}I]-T3 in the presence or absence of NADPH and/or unlabeled T3 for 20 min on ice. After the brief incubation with charcoal and the following centrifugation, the supernatant and pellet were counted by the γ-counter.

Heart rate

For the ECG measurements, mice were anesthetized either with ketamine (100 mg/kg) and xylazine (10 mg/kg) via intraperitoneal injection as described previously (31). Briefly, mice were positioned prone in a shielded box. The bottom of the shielded box was heated to 37 °C using a heating pad to maintain a stable body temperature during the experiment. UAS-108S (Unique Medical, Tokyo) was used to record bipolar limb leads in standard fashion. For each animal, R-R intervals were measured in a blinded fashion from three consecutive beats in the leads and averaged.

Measurement of serum T3 and T4

Four hundred μl of peripheral blood was corrected from the six-week old male mouse. Serum T3 and T4 were measured by Chemilumi ACS-T3, T4 (Bayer Med, Tokyo). Six of individual mouse in each genotype group were used in the study.

Auditory-Evoked Brainstem Response (ABR)

The chimeric mouse was mated to 129Sv mice and then back-crossed 6 times into the same strain, diluting the C57BL6 background. Six-week old male mice

were used in this study. Mice were anesthetized with ketamine (100mg/kg) / xylazine (10mg/kg) by intraperitoneal injection and the ABR tests were performed with a heating pad to maintain the body temperature in a soundproof room as previously described (32). Click stimuli was performed at synthesized durations and specified amplitudes using a digital signal processing platform (Tucker-Davis Technologies, FL, USA), and analyzed with PowerLab systems (ADInstruments, Australia) as described (33). Click stimuli were 0.1ms clicks, composed of a square pulse of 0.1ms duration. Stainless steel needle electrodes were placed at the vertex and ventrolateral to the left and right ears for the recording and a tweeter modified with a coupler was inserted into the external canal to deliver acoustic stimuli. ABR waveforms were recorded in 5-10dB intervals down from a maximum amplitude of 85dB until no waveform could be visualized.

Measurement of TSHβ, glutathione S transferase alpha 2 (Gsta2) and deiodinase 1 (Dio1)

The contents of TSHβ, Gsta2 and Dio1 were measured as follows. After injection with ice cold PBS intravenously, pituitary glands, livers and kidneys were removed and washed with RNA later (Qiagen, CA). Total RNA was prepared by using RNeasy kit (Qiagen, CA). After reverse transcription with AMV-RT, samples were applied with Quantitect SYBR Green PCR kit (Qiagen, CA) or TaqMan universal PCR Master Mix to ABI PRISM 7300 Sequence detection system according to a manufacturer's protocol. Mouse TSHβ, β-actin, Dio1 and Gsta2, were measured with the following oligonucleotides.

TSHβ sense 5'-GCTCGGGTTGTTCAAAGCATGA-3'
antisense 5'-CCCACAAGCAAGAGCAAAAAGCA-3'
β-actin sense 5'-TCTCCAGAGGCACCATTGAAATTCT-3'
antisense 5'-CGCTGGCTCCCACCTTGTCT-3'
Dio1 sense 5'-CCAGTTCAAGAGACTCGTAGATGAC-3'
Antisense 5'-GCGTGAGCTTCTTCAATGTAAATGA-3'
FAM-TCCACAGCCCATTTC-3'
Gsta2 sense 5'-AAGACTACCTTGTGGGCAACAG-3'
Antisense 5'-CTGGCATCAAGCTCTTCAACATAGA-3'

FAM-CCTGCTGGAACTTC-3’

The amount of 18s ribosomal RNA was measured as described in the manufacturer’s protocol using commercially available probes (Applied Biosystems, Foster City, CA).

Tracer experiments

Mice were kept under a 12-hour light cycle and provided food and water *ad libitum*. Three or four CRYM+/+ and three CRYM-/- male littermates were used for each group of treatment. Each mouse was injected intravenously with 0.2μCi (91pmol) of [^{125}I]T3 dissolved into 50μl of saline. At 1,2,4, and 8 hours after injection, the mice were sacrificed and removed the tissues, following which the blood samples were drawn. Each tissue and blood sample were evaluated radioactivity with γ-counter after measurement of the weight.

Statistics

In Fig2d and 5, *P* values were calculated by an analysis of variance (ANOVA) unpaired *t* test using the Statview 4.1 software (Abacus, Berkely, CA). In Fig3 and 4, statistical significance was determined by an ANOVA followed by the *Bonferroni* multiple comparison test. *P* values $\geq$ 0.05 were considered not significant.

Acknowledgement

We thank Ms. Izumi Kinoshita for her technical assistance. We are also grateful to Ms. Tomoko Nishizawa for preparation of the tissues. This work was supported in part by a Grant-in-Aid for Scientific Research No. 17590957 from the Ministry of Education, Science, Sports, and Culture, Japan.

References

1. **Flamant F, Gauthier K, Samarut J** 2006 Thyroid hormone signaling is getting more complex: STORMs are coming. Mol Endocrinol Epub ahead of print
2. **Lazar MA** 1993 Thyroid hormone receptors: multiple forms, multiple possibilities. Endocr Rev 14: 184-193
3. **Friesema EC, Jansen J, Milici C, Visser TJ** 2005 Thyroid hormone transporters. Vitam Horm 70: 137-167
4. **Ichikawa K Hashizume K** 1995 Thyroid hormone action in the cell. Endocr J 42: 131-140
5. **Hashizume K, Kobayashi M, Miyamoto T** 1986 Active and inactive forms of 3,5,3'-triiodo-L-thyronine (T3)-binding protein in rat kidney cytosol: possible role of nicotinamide adenine dinucleotide phosphate in activation of T3 binding. Endocrinology 119: 710-719
6. **Hashizume K, Miyamoto T, Ichikawa K, Yamauchi K, Kobayashi M, Sakurai A, Ohtsuka H, Nishii Y, Yamada T** 1989 Purification and characterization of NADPH-dependent cytosolic 3,5,3'-triiodo-L-thyronine binding protein in rat kidney. J Biol Chem 264: 4857-4863
7. **Lennon AM** 1992 Purification and characterization of rat brain cytosolic 3,5,3'-triiodo-L-thyronine-binding protein. Evidence for binding activity dependent on NADPH, NADP and thioredoxin Eur J Biochem 210: 79-85
8. **Kobayashi M, Hashizume K, Suzuki S, Ichikawa K, Takeda T** 1991 A novel NADPH-dependent cytosolic 3,5,3'-triiodo-L-thyronine-binding protein (CTBP;5.1S) in rat liver: a comparison with 4.7S NADPH-dependent CTBP. Endocrinology 129: 1701-1708
9. **Beslin A, Vié MP, Blondeau JP, Francon J** 1995 Identification by photoaffinity labeling of a pyridine nucleotide-dependent tri-iodothyronine-binding protein in the cytosol of cultured astroglial cells. Biochem J 305: 729-737
10. **Vié MP, Blanchet P, Samson M, Francon J, Blondeau JP** 1996 High affinity thyroid hormone-binding protein in human kidney: kinetic characterization and identification by photoaffinity labeling. Endocrinology 137: 4563-4570
11. **Kim RY, Gasser R, Wistow GJ** 1992 μ-crystallin is a mammalian

homologue of Agrobacterium ornithine cyclodeaminase and is expressed in human retina. Proc Natl Acad Sci USA 89: 9292-9296

12. **Vié MP, Evrard C, Osty J, Breton-Gilet A, Blanchet P, Pomerance M, Rouget P, Francon J, Blondeau JP** 1997 Purification, molecular cloning, and functional expression of the human nicotinamide-adenine dinucleotide phosphate-regulated thyroid hormone binding protein. Mol Endocrinol 11: 1728-1736
13. **Wistow G, Kim H** 1991 Lens protein expression in mammals: taxon-specificity and the recruitment of crystallins. J Mol Evolution 32: 262-269
14. **Mori J, Suzuki S, Kobayashi M, Inagaki T, Komatsu A, Takeda T, Miyamoto T, Ichikawa K, Hashizume K** 2002 Nicotinamide adenine dinucleotide phosphate-dependent cytosolic T3 binding protein as a regulator for T3-mediated transactivation. Endocrinology 143: 1538-1544
15. **Abe S, Katagiri T, Saito-Hisaminato A, Usami S, Inoue Y, Tsunoda T, Nakamura Y** 2003 Identification of CRYM as a candidate responsible for nonsyndromic deafness, through cDNA microarray analysis of human cochlear and vestibular tissues. Am J Hum Genet 72: 73-82
16. **Oshima A, Suzuki S, Takumi Y, Hashizume K, Abe S, Usami S** 2006 CRYM mutations cause deafenss through thyroid hormone binding properties in the fibrocytes of the cochlea. J Med Genet 43: e25
17. **Suzuki S, Hashizume K, Ichikawa K, Takeda T** 1991 Ontogenesis of the high affinity NADPH-dependent cytosolic 3,5,3'-triiodo-L-thyronine-binding protein in rat. Endocrinology 129: 2571-2574
18. **Krueger KE, Srivastava S** 2006 Posttranslational protein modifications: Current implications for cancer detection, prevention, and therapeutics. Mol Cell Proteomics 10: 1799 -1810
19. **Meyerhoff WL** 1979 Hypothyroidism and the ear: electrophysiological, morphological, and chemical considerations. Laryngoscope 89: 1-25
20. **Knipper M, Zinn C, Maier H, Praetorius M, Rohbock K, Kopschall I, Zimmermann U** 2000 Thyroid hormone deficiency before the onset of hearing causes irreversible damage to peripheral and central auditory systems. J Neurophysiol 85: 3101-3112

21. **Sadow PM, Chassande O, Gauthier K, Samarut J, Xu J, O'Malley BW, Weiss RE** 2003 Specificity of thyroid hormone receptor subtype and steroid receptor coactivator-1 on thyroid hormone action. Am J Physiol Endocrinol Metab 284: E36-46

22. **Bianco AC, Salvatore D, Gereben B, Berry MJ, Larsen PR** 2002 Biochemistry, cellular and molecular biology, and physiological roles of the iodothyronine selenodeiodinases. Endocr Rev 23: 38-89

23. **Ashizawa K, Cheng S-y** 1992 Regulation of thyroid hormone receptor-mediated transcription by a cytosol protein. Proc Natl Acad Sci USA 89: 9277-9281

24. **Yamauchi K, Nakajima J, Hayashi H, Horiuchi R, Tata JR** 1999 Xenopus cytosolic thyroid hormone-binding protein (xCTBP) is aldehyde dehydrogenese catalyzing the formation of retinoic acid. J Biol Chem 274: 8460-8469

25. **Ishigaki S, Abramovitz M, Listowsky I** 1989 Glutathione-S-transferases are major cytosolic thyroid hormone binding proteins. Arch Biochem Biophys 273: 265-272

26. **Goodman JL, Wang S, Alam S, Ruzicka FJ, Frey PA, Wedekind JE** 2004 Ornithine Cyclodeaminase: structure, mechanism of action, and implications for the μ-crystallin family. Biochemistry 43: 13883-13891

27. **Suzuki S, Mori J, Kobayashi M, Inagaki T, Inaba H, Komatsu A, Yamashita K, Takeda T, Miyamoto T, Ichikawa K, Hashizume K** 2003 Cell-specific expression of NADPH-dependent cytosolic 3,5,3'-triiodo-L-thyronine-binding protein (p38CTBP). Eur J Endocrinol 148: 259-268

28. **Hashizume K, Miyamoto T, Ichikawa K, Yamauchi K, Sakurai A, Ohtsuka H, Kobayashi M, Nishii Y, Yamada T** 1989 Evidence for the presence of two active forms of cytosolic 3,5,3'-triiodo-L-thyronine-binding protein (CTBP) in rat kidney. Specialized functions of two CTBPs in intracellular T3 transactivation. J Biol Chem 264: 4864-4871

29. **Knollmann BC, Blatt SA, Horton K, de Freitas F, Miller T, Bell M, Housmans PR, Weissman NJ, Morad M, Potter JD** 2001 Inotropic stimulation induces cardiac dysfunction in transgenic mice expressing a

troponin T (I79N) mutation linked to familial hypertrophic cardiomyopathy. J Biol Chem 276:10039–10048

30. **Szymko-Bennett YM, Kurima K, Olsen B, Seegmiller R, Griffith AJ** 2003 Auditory function associated with *Col11a1* haploinsufficiency in chondrodysplasia (cho) mice. Hearing Res 175: 178-182

31. **Suzuki N, Asamura K, Kikuchi Y, Takumi Y, Abe S, Imamura Y, Hayashi T, Aszodi A, Fässler R, Usami S** 2005 Type IX collagen knock-out mouse shows progressive hearing loss. Neurosci Res 51: 293-298

Figure Legends

Fig1

a. Schematic representation of the *CRYM* gene and targeting.

Exon1 and Exon2 were disrupted by the substitution for neomycin resistance (NeoR) gene driven by mouse phosphoglycerate kinase promoter and polyA tail. The long fragment of the targeting construct was a 7.3-kilobase sequence upstream from Exon1. The short fragment of the targeting construct was 1.2-kilobase-long sequence downstream of Exon2. LA; long arm, SA; short arm.

b. the expressions of the CRYM mRNA and protein.

(*left panel*) Total RNA was extracted from the brain in 3-week-old wild, CRYM+/-, and CRYM-/- mice. Blotting membrane was hybridized with ^{32}P-dCTP labeled whole cDNA of the CRYM as a probe. (*right panel*) Cell lysate was prepared and applied to 10% SDS-polyacrylamide gel. The blotting membrane was incubated with anti-μ-crystallin antibody (L-20) (Santacruz, CA). Detection was carried out by measuring the enhanced chemiluminescence using horseradish peroxidase-coupled rabbit anti-goat IgG antibody (Amersham Bioscience). (+/+; wild mice, +/-; CRYM+/-, -/-: CRYM-/-)

c. Specific T3 binding in the brain, heart, kidney and liver of CRYM+/+ and CRYM-/- mice.

After the tissues were removed from the CRYM+/+ or CRYM-/- mice, crude cytosol fractions were prepared and were incubated with 1% (w/v) charcoal for 20 min. After spinning down, the supernatants were incubated with labeled T3 in the presence or absence of NADPH, with or without 10^{-6}M unlabeled T3 for 20 min. After the incubation, dextran-coated charcoal was added, incubated for a few seconds, and spinned down to remove charcoal. The supernatant was taken to count the radioactivity. (+/+; CRYM+/+, -/-: CRYM-/-) “NADPH - and +” denote the incubation without and with 100μM NADPH, respectively. “T3 – and +” indicate the incubation without and with unlabeled 10^{-6}M T3, respectively.

d. Scatchard analysis of the kidney cytosol obtained from the CRYM+/+ and CRYM-/- mice.

The charcoal treated cytosol was incubated with labeled T3 in the

various concentration of unlabeled T3 to perform Scatchard analysis. +/+ represents the analysis of the CRYM+/+ mice. -/- shows the analysis of the CRYM-/- mice. The representative data were shown.

Fig2

a. Growth rate of CRYM+/+, CRYM+/-, and CRYM-/- mice. The data represent mean of three or four male mice ± SD.

b. Heart rate of the CRYM+/+, CRYM+/-. and CRYM-/- mice. Three-week-old male mice were anesthetized and recorded by the electrocardiogram. The data obtained from CRYM+/+ mice treated with low iodide diet plus 0.1% PTU (LID+PTU) and 1μg/ml water *ad libitum* (T3 water) were shown in the first and second column, respectively. Numbers in parentheses indicate numbers of animals studied.

c. Auditory-evoked brainstem response in CRYM+/+ and CRYM-/- mice.

The chimeric mouse was mated to 129Sv mice and then back-crossed 6 times into the same strain, diluting the C57BL6 background. Six-week old male mice were used in this study. The representative data were shown.

d. The thresholds of CRYM-/- mice were not significantly different from CRYM+/+ mice.

The data were obtained from six-week old male mice. ABR waveforms were recorded in 5-10dB intervals down from a maximum amplitude of 85dB until no waveform could be visualized. A threshold was defined as the minimal stimulus level that gave a recognizable waveform on a normalized scale. The data represent mean ± SD of six determinations. NS; not significant

Fig3

a. Serum concentrations of T3 and T4 and the expression of TSHβ mRNA in 3-week old male mice.

After drawing the blood for the measurement of thyroid hormone, mice were anesthetized with ketamine/xylazyne, and infused ice-cold saline from the aorta. The pituitary glands were taken and extracted the total RNA. The TSHβ and β-actin were quantitated by PCR. All values corrected by the amount of β-actin. Columns indicated mean ± SD from six individual determinations. *; $P<0.05$, **;

P<0.01

b. Northern blotting of TSHβ expression in the pituitary glands obtained from CRYM+/+ and CRYM -/- mice.

Six-week-old male mice were used. Ten μg of total RNA obtained from six mice was loaded and hybridized with labeled TSHβ or EF1 as an internal control.

c. Histology of the pituitary gland and the thyroid gland in CRYM+/+ and CRYM-/- mice.

Eight-week-old male mice were used. Sections were stained with hematoxylin and eosin. The pituitary glands in CRYM +/+ and CRYM-/- mice were shown in *left upper panel* and *right upper panel*, respectively. The thyroid glands in CRYM +/+ and CRYM-/- were shown in *left lower panel* and *right lower panel*, respectively. There are no apparent differences in both tissues in both genotypes.

Fig4 The expressions of Gsta2 and Dio1 mRNA in liver, kidney and heart of CRYM+/+, CRYM+/- and CRYM-/- mice.

a. Tissues were removed after saline infusion. Fifty mg of each tissues were homogenized and extracted the total RNA. Twenty ng of each purified total RNA was used for reverse-transcription. The mRNAs of Gsta2 and Dio1 were quantitated by sequence detection system. All values were corrected by the amount of 18s ribosomal RNA. The column indicate mean $\pm$ SD from four individual determinations. The expression level of Gsta2 in heart was too low to measure in this system.

b. Northern blotting of Dio1 and Gsta2 expressions in liver and kidney obtained from CRYM+/+. CRYM+/-, and CRYM-/- mice.

Six-week-old male mice were used. Twenty μg of total RNA obtained from the tissues in CRYM+/+, CRYM+/-, or CRYM-/- mice was loaded and hybridized with labeled Dio1 or Gsta2. Elongation factor1 (EF1) was used as an internal control.

Fig5 Radioactivity of the tissues removed from wild (CRYM+/+) and homozygous knockout (CRYM-/-) mice at the indicated hours after the injection of [^{125}I]T3.

Six-week old mice were intravenously injected 91pmol [^{125}I]-T3 via the tail vein. Tissues and blood samples were removed from three or four of each at the indicated times after the injection. After the measurement of the tissue weight, radioactivities were counted. The data indicated mean $\pm$ SD. (a; brain, b; heart, c; liver, d; kidney, e; blood) *, $P<0.01$ vs. study with CRYM+/+ mice.

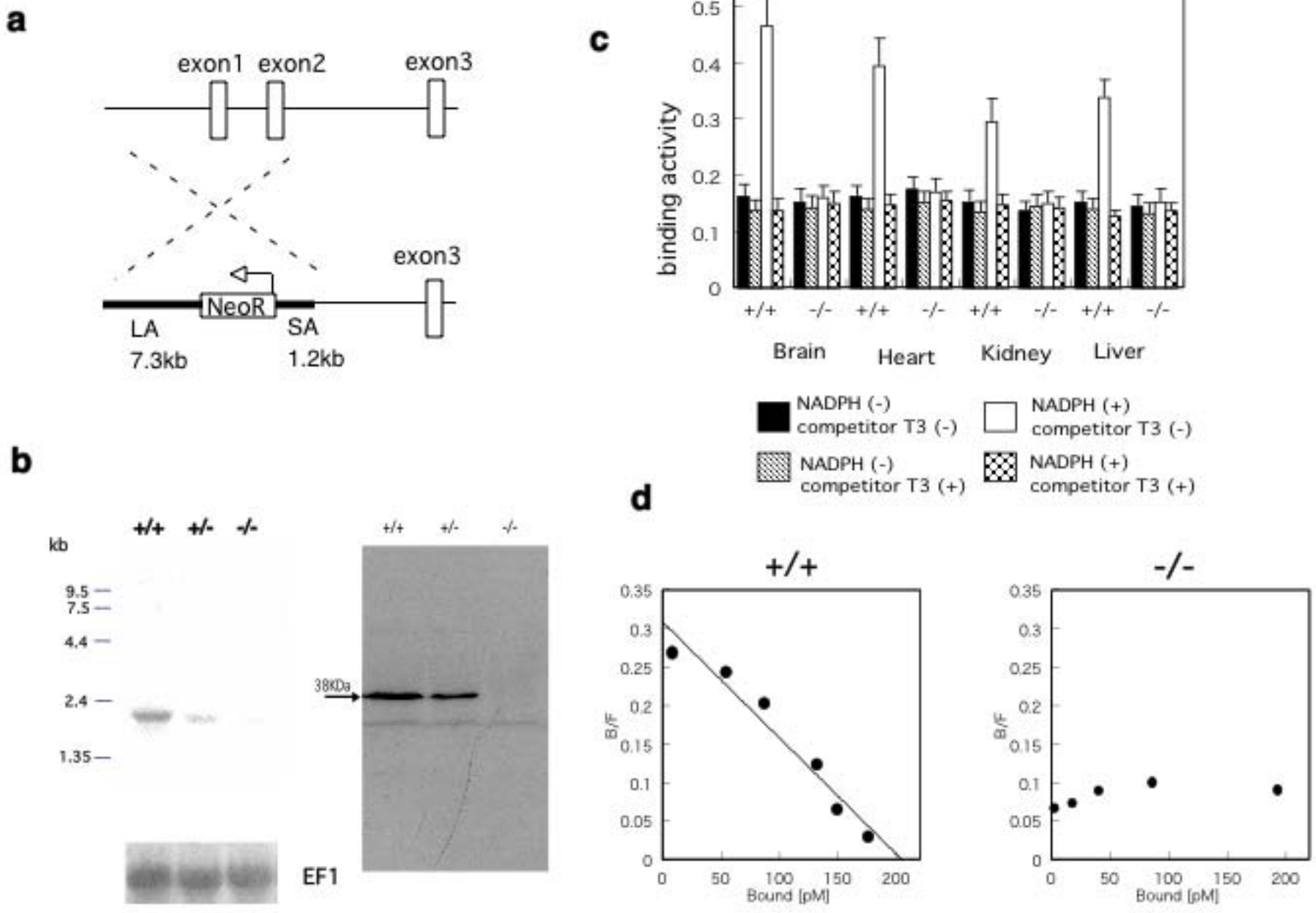
a
exon1
exon2
exon3
exon3
NeoR
LA
7.3kb
SA
1.2kb
b
+/+
+/-
-/-
kb
9.5
7.5
4.4
2.4
1.35
+/+
+/-
-/-
38KDa
EF1
c
binding activity
0.5
0.4
0.3
0.2
0.1
0
+/+
-/-
+/+
-/-
+/+
-/-
+/+
-/-
Brain
Heart
Kidney
Liver
NADPH (-)
competitor T3 (-)
NADPH (+)
competitor T3 (-)
NADPH (-)
competitor T3 (+)
NADPH (+)
competitor T3 (+)
d
+/+
-/-
B/F
Bound [pM]
0.35
0.3
0.25
0.2
0.15
0.1
0.05
0
0
50
100
150
200

Fig1

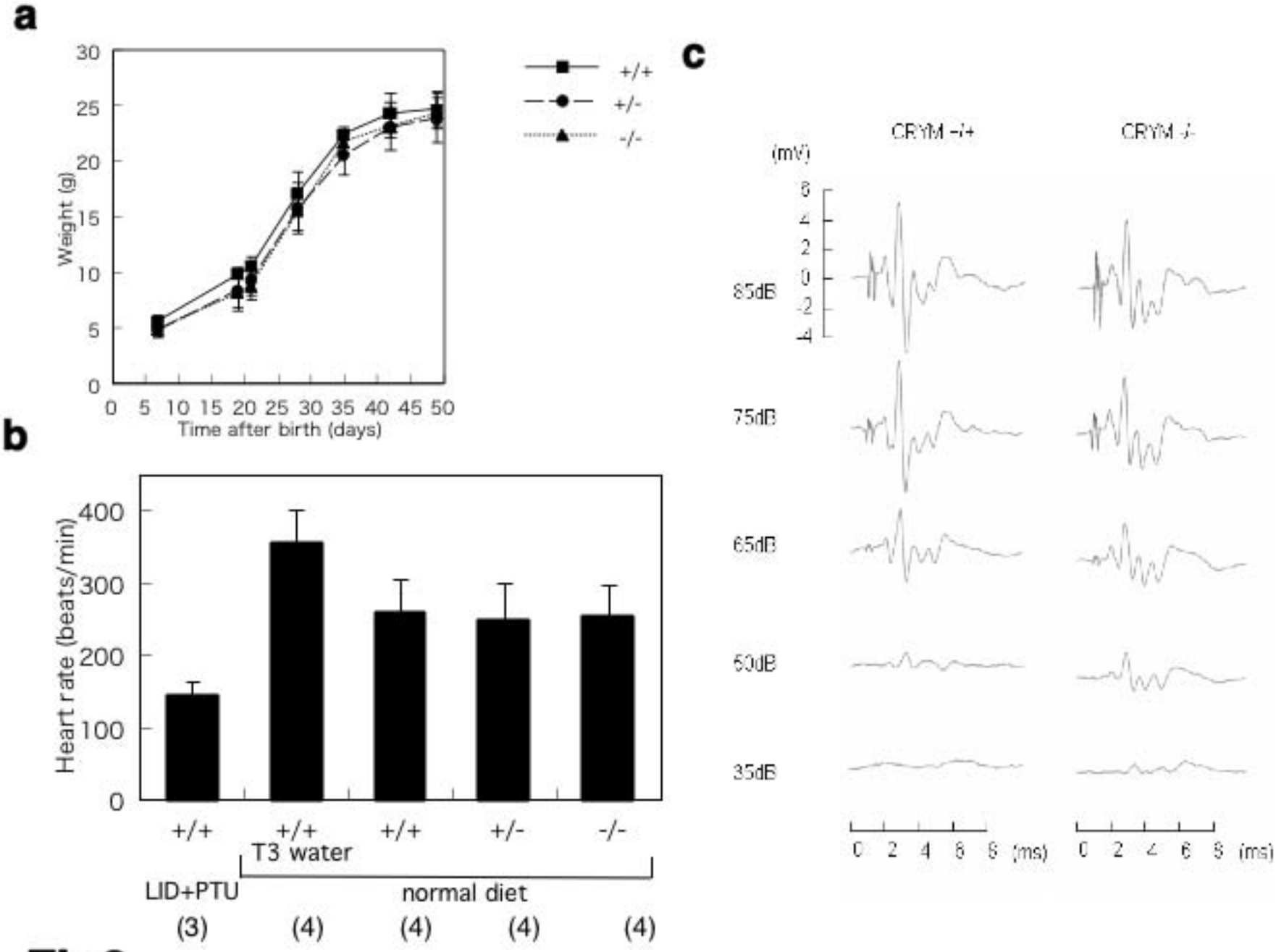
a
Weight (g)
Time after birth (days)
+/+
+/-
-/-
b
Heart rate (beats/min)
+/+
+/+
+/+
+/-
-/-
T3 water
LID+PTU
normal diet
(3)
(4)
(4)
(4)
(4)
c
CRYM -/+
CRYM -/-
(mV)
85dB
75dB
65dB
55dB
35dB
(ms)
(ms)

Fig2

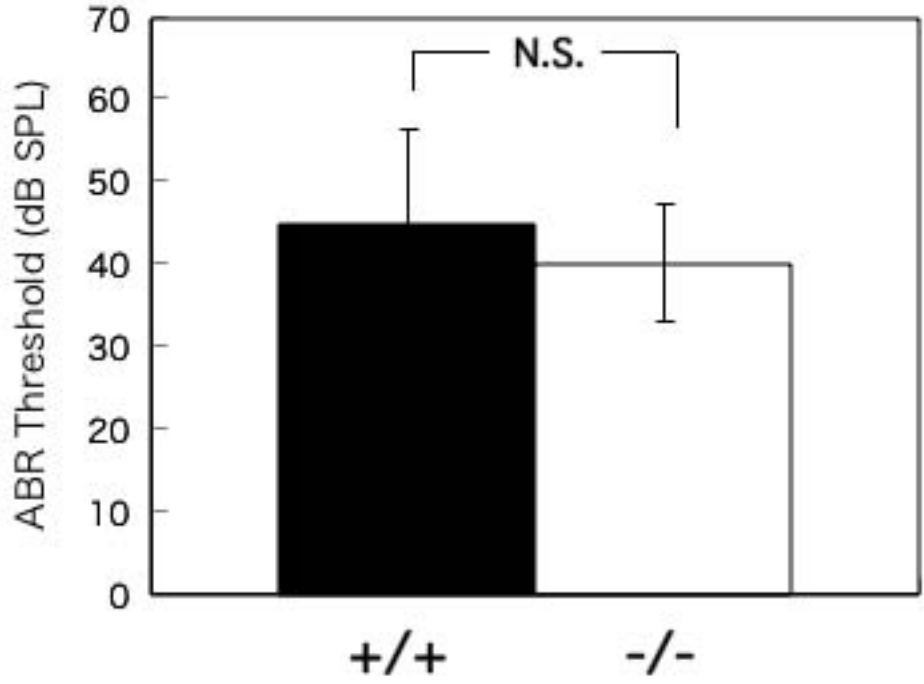

Fig 2d

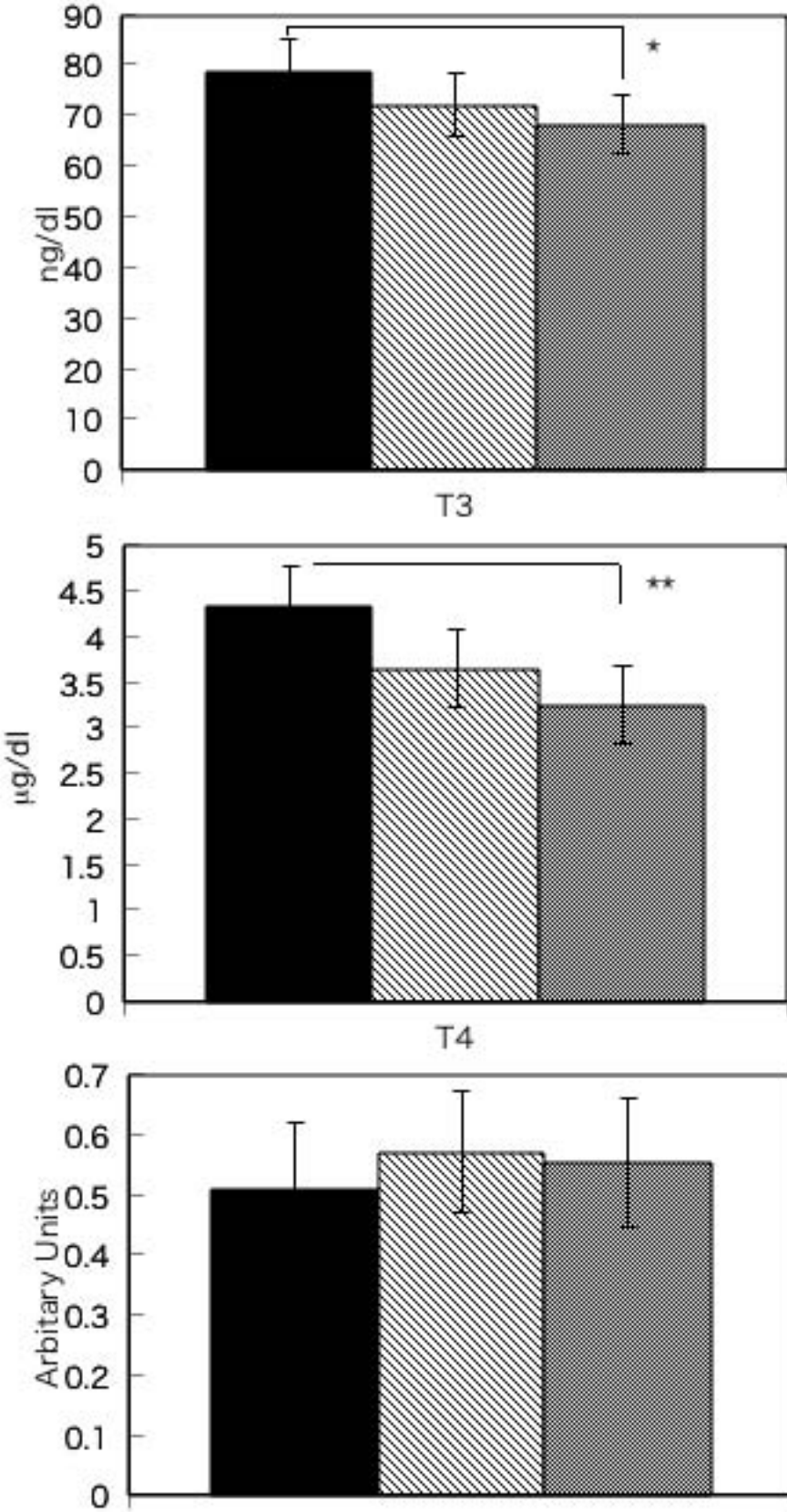
90
80
70
60
50
40
30
20
10
0
ng/dl
*
T3
5
4.5
4
3.5
3
2.5
2
1.5
1
0.5
0
μg/dl
**
T4
0.7
0.6
0.5
0.4
0.3
0.2
0.1
0
Arbitary Units
TSHβ
+/+
+/-
-/-

Fig3 a

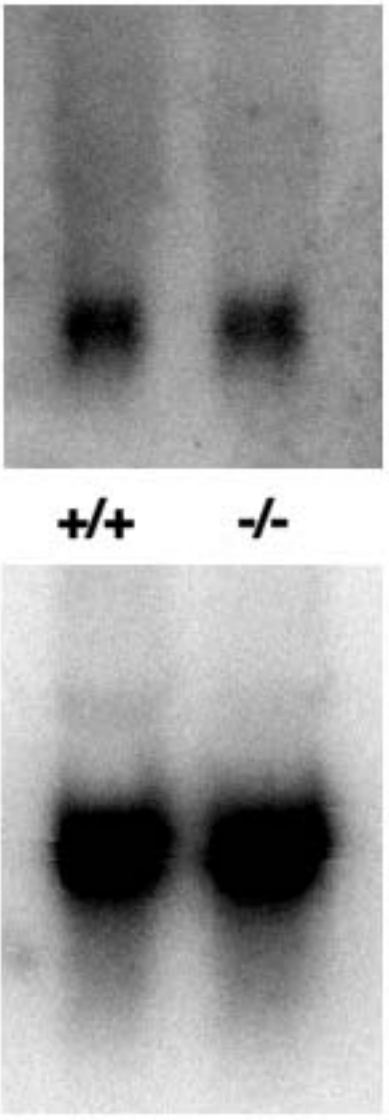

Fig3 b

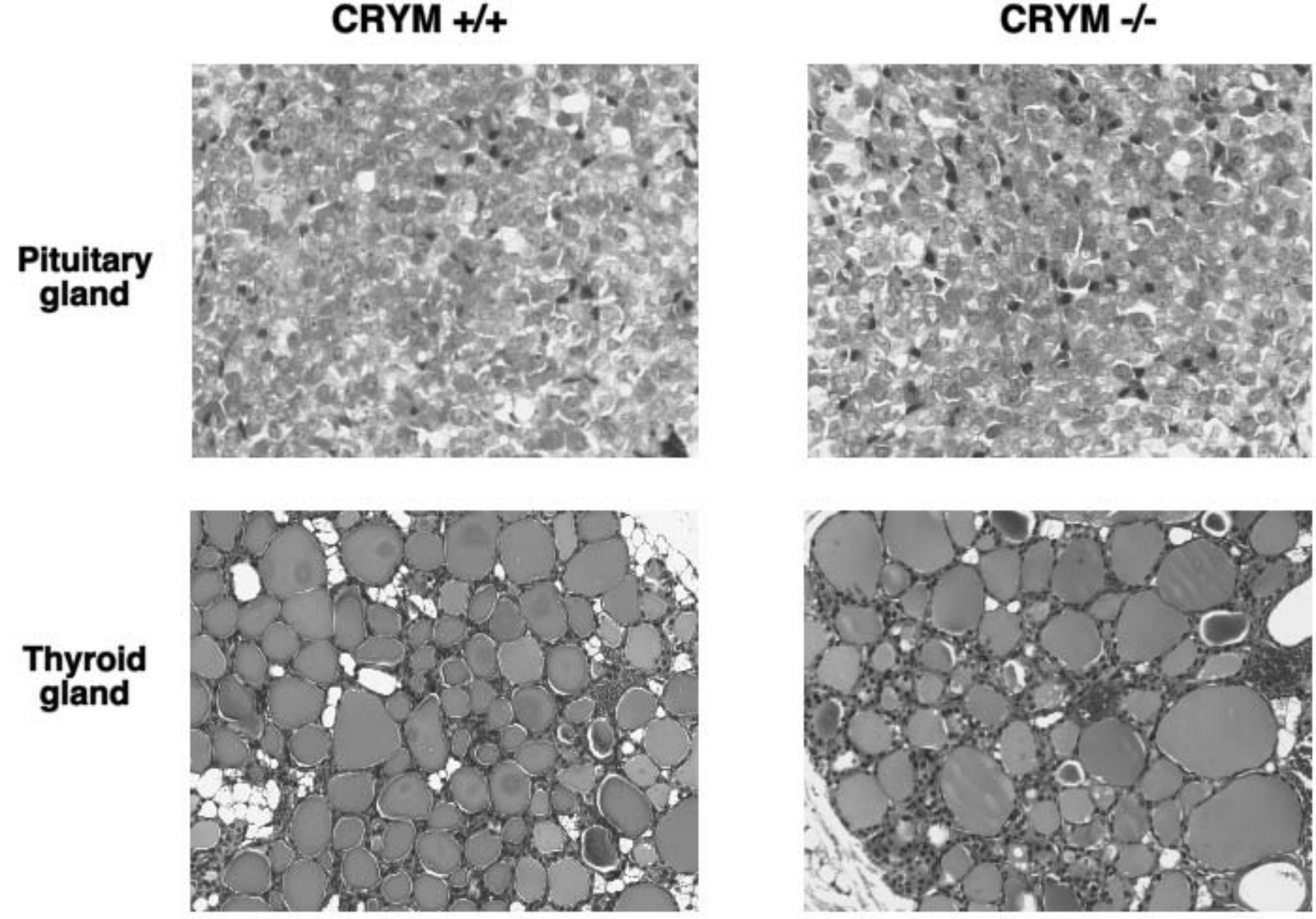

Fig3 c

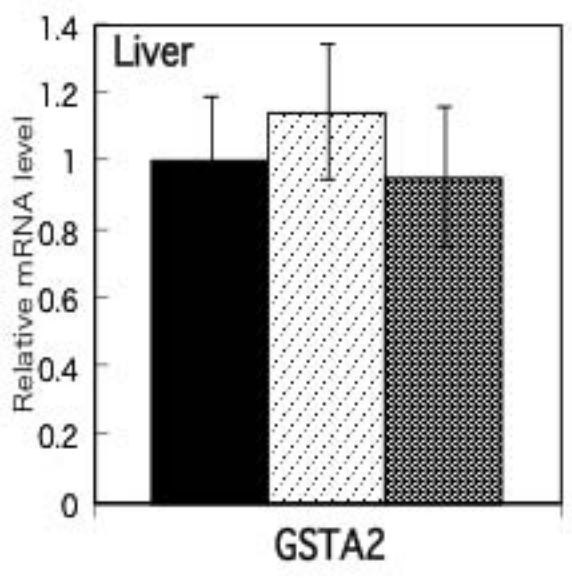
Liver
Relative mRNA level
1.4
1.2
1
0.8
0.6
0.4
0.2
0
GSTA2

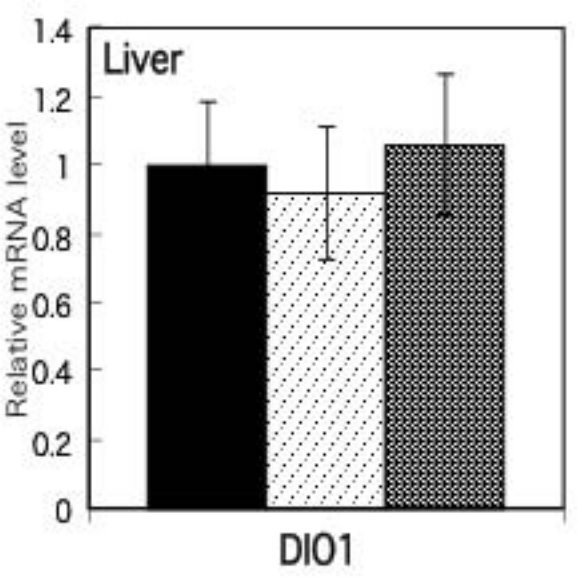
Liver
Relative mRNA level
1.4
1.2
1
0.8
0.6
0.4
0.2
0
DIO1

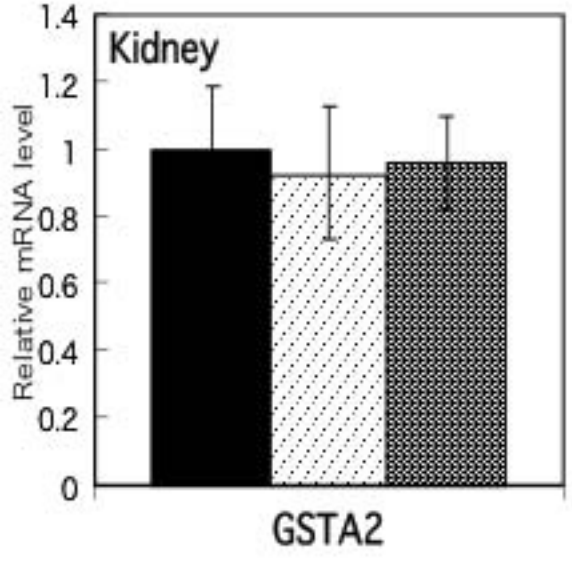
Kidney
Relative mRNA level
1.4
1.2
1
0.8
0.6
0.4
0.2
0
GSTA2

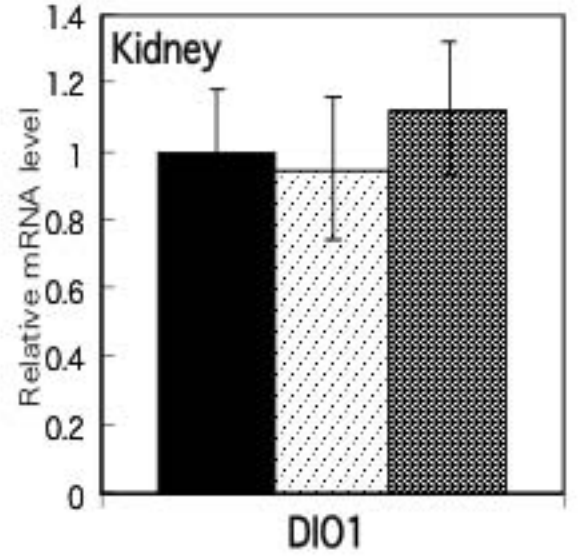
Kidney
Relative mRNA level
1.4
1.2
1
0.8
0.6
0.4
0.2
0
DIO1

Fig4 a

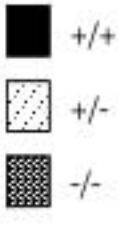
+/+
+/-
-/-

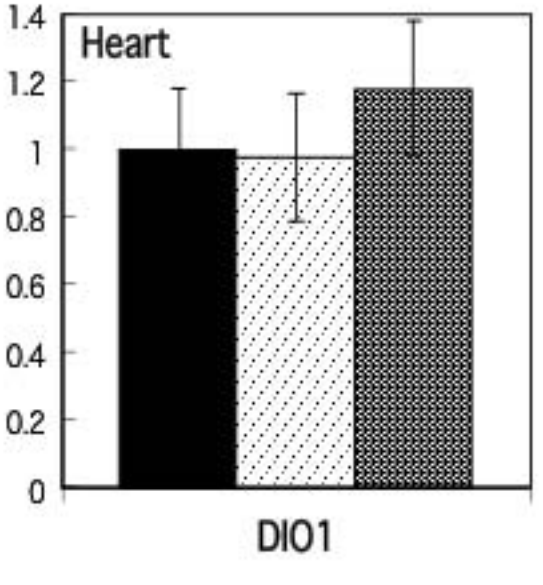
Heart
1.4
1.2
1
0.8
0.6
0.4
0.2
0
DIO1

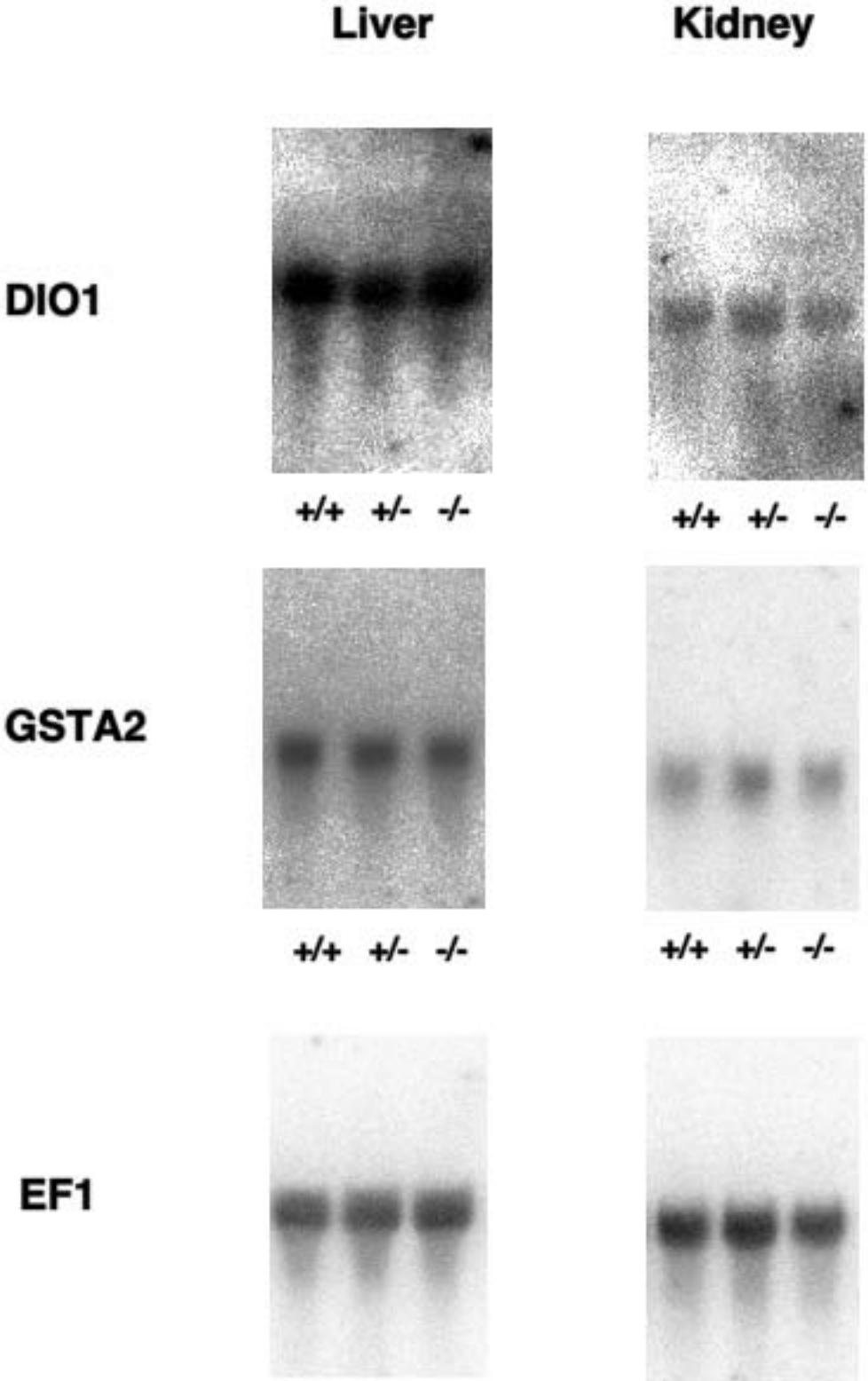

Fig4 b

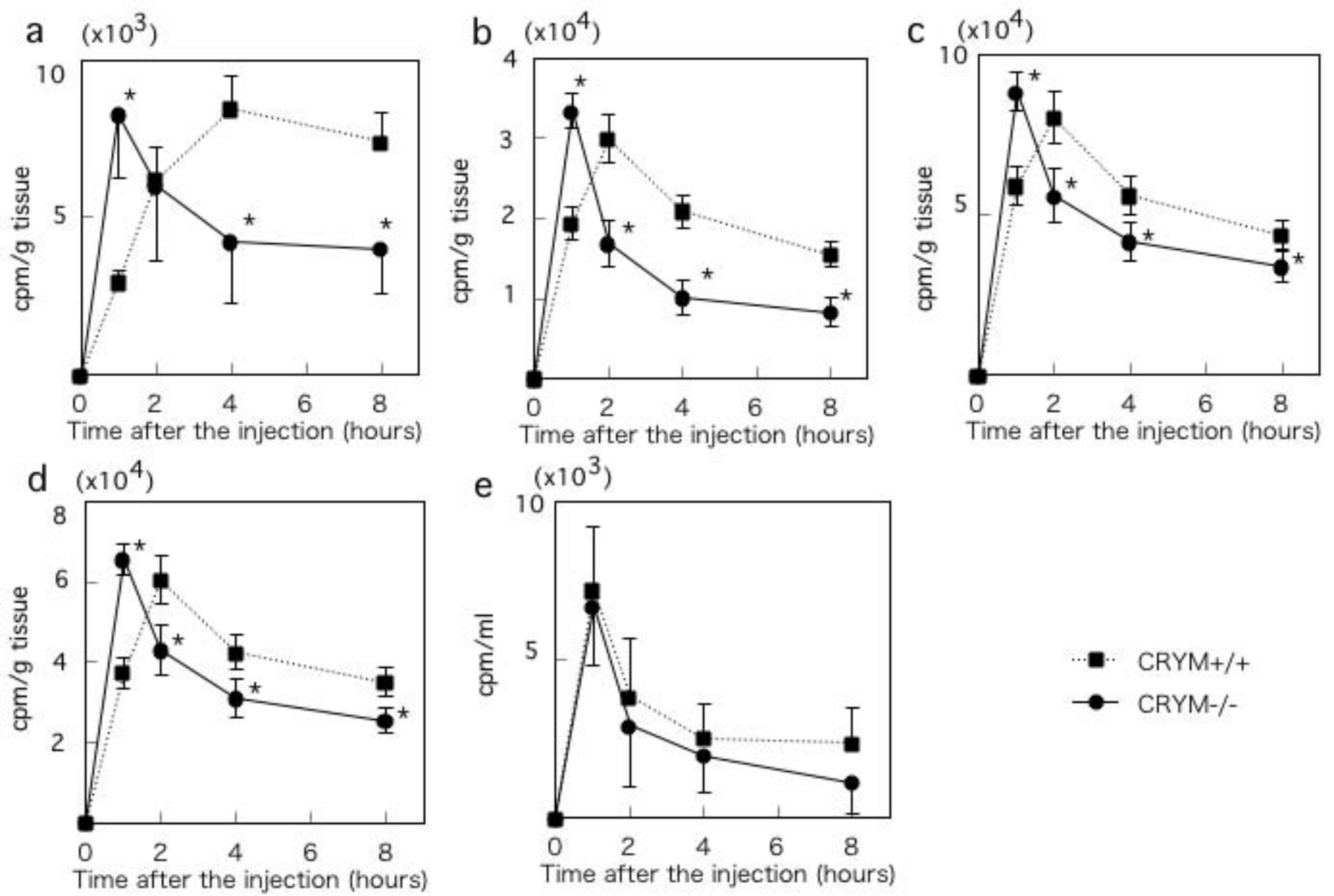
a
(x10^3)
10
5
cpm/g tissue
0
2
4
6
8
Time after the injection (hours)
b
(x10^4)
4
3
2
1
cpm/g tissue
Time after the injection (hours)
c
(x10^4)
10
5
cpm/g tissue
Time after the injection (hours)
d
(x10^4)
8
6
4
2
cpm/g tissue
Time after the injection (hours)
e
(x10^3)
10
5
cpm/ml
Time after the injection (hours)
CRYM+/+
CRYM-/-

Fig5